Evaluation of a district cooling network using R-744 as the energy carrier: A case study

Pedersen, Rikke C.; Worm, Jakob ; Reinholdt, Lars ; Elmegaard, Brian; Arabkoohsar, Ahmad

Published in:
Proceedings of ECOS 2024 - The 37th International Conference on Efficiency, Cost, Optimization, Simulation and Environmental Impact of Energy Systems 2024

Link to article, DOI:
10.52202/077185-0075

Publication date:
2024

Document Version
Publisher's PDF, also known as Version of record

Evaluation of a district cooling network using R-744 as the energy carrier: A case study

Rikke C. Pedersen [a]*, Jakob Worm [b], Lars Reinholdt [b], Brian Elmegaard [a] and Ahmad Arabkoohsar [a]

[a] Technical University of Denmark, Dept. of Civil & Mechanical Eng., Kgs. Lyngby, DK

[b] PlanEnergi, Aarhus, DK

*Corresponding Author: rikpe@dtu.dk

ABSTRACT

Due to the increase in global temperatures, there is a need to provide more efficient district cooling systems in the future. In this study, a district cooling system using R-744 as the energy carrier was used to provide comfort cooling at five commercial buildings located in Denmark. The heat of the network was utilised to produce district heating in the local network using a heat pump. Two alternative system designs and operation strategies for the pressure levels throughout the network were analysed and compared on the energy performance. It was found that a system with lower temperature levels and direct cooling at the consumer substations required smaller pipes in the forward line but showed an overall slight increase in power consumption. This was caused by the reduced performance of the central heat pump. The results show, that the operating strategy of pressure levels in the system should be chosen not only to optimise the consumer substation but should also consider the operation of the central heat pump, as this is an important component of both operation and capital expenses.

1 INTRODUCTION

The global temperature has been rising for decades caused by an increased concentration of greenhouse gases in the atmosphere. In 2023, the average global temperature was 1 °C greater than the average between 1961-1990 (Intergovernmental Panel on Climate Change, 2022). As the temperature rises, the need for comfort cooling also increases. Cooling is the fastest-growing use of energy in buildings, and with the current path, the electricity demand for comfort cooling in 2050 will be more than three times the demand of today (IEA, 2018). In 2016, the energy use in buildings accounted for approximately 18 % of the global greenhouse gas emissions (Ritchie & Roser, 2020), therefore, it is of major importance, that future needs for comfort cooling can be provided more efficiently with less environmental impact.

In urban and densely populated areas, one solution is to implement district cooling networks which supply energy to buildings in a centralized and efficient way (IEA, 2018). However, it is challenging to construct new energy networks in well-established urban areas, as there can be interference with important infrastructure during the construction period and because the space within the ground can be limited (Henchoz *et al.*, 2015). Conventional district energy systems utilize water as the energy carrier, but an alternative system using the refrigerant R-744 (CO_2) was proposed by Weber and Favrat (2010). In the R-744 system, the latent heat of vaporization and condensation is utilised for heat transfer as opposed to sensible heat in conventional water based systems. The system requires only two pipes, one for liquid and gaseous refrigerant, respectively. This allows for smaller mass flow rates of the energy carrier and thereby reduces the pipe sizes which can result in reduced construction time and costs and will occupy less space within the ground (Henchoz *et al.*, 2016). The concept was analysed by Weber and Favrat (2010) and the exergetic and economic performance was compared to that of

a conventional water based system. They find that the R-744 system can reduce costs by 12 % and improve exergy performance. Henchoz *et al.* (2015) evaluate the benefit of implementing a R-744 based district energy system in a small urban area and find that electricity and fuel consumption is reduced by more than 80 % while the economy is significantly improved compared to the existing system consisting of individual heating and cooling units. The refrigerant based system is a new concept, therefore, several challenges and concerns exist. These are discussed by Henchoz *et al.* (2016). One aspect is the relatively high pressure level of the R-744 system (ranging between 40 bar to 60 bar depending on temperature levels). They find that regulations become stricter with higher pressure levels and they also suggest safety measures regarding potential leakages. A small scale test setup was made by Henchoz *et al.* (2017) which shows that control strategies can be implemented for such system, reducing the safety concerns. Nagano *et al.* (2021) investigate the use of an R-744 based district energy system in an urban area with different natural available thermal reservoirs. They consider different network configurations and find that the temperature level throughout the network should be optimised with respect to the thermal reservoir and vary over the year to achieve the lowest energy consumption. However, it is suggested by Henchoz *et al.* (2015) that the temperature level of the network should be set to allow for direct cooling at consumer substations.

In this study, a district cooling network using R-744 as the energy carrier was investigated. A case was considered, where five commercial buildings were supplied with comfort cooling. The heat was discharged to the local district heat network through a centralised heat pump. Two alternative system designs and operation strategies (OP) for choosing the pressures of the network were compared. In the first case (OP-HP), the pressure varied over the year so that R-744 operated close to ambient temperatures. Heat pumps (HP) were used at the consumers to provide cooling at adequate temperatures. In the second case (OP-DC), the pressure was set to provide direct cooling (DC) at the consumers. A thermodynamic model of the system was made, and the required dimensions of pipelines were determined. The yearly power consumption, district heat production, and network losses were compared for the two cases to identify the trade-offs between these performance parameters.

2 METHODS

2.1 Case description

A district cooling network with five consumers was considered. The consumers are commercial buildings and have a space cooling need throughout the year. The cooling network was constructed so that the consumers were all connected to the same string with consumer five being the last consumer on the string (Figure 1). The peak consumptions and the distance to each consumer (measured from the previous consumer) are listed in Table 1.

A linear relation between the cooling demand and ambient temperature was assumed, so that the peak demand occurred in the hour with the maximum temperature of the year (24 °C). In the investigated case, cooling was provided in hours with ambient temperatures of $T \geq 11\,°\mathrm{C}$, corresponding to 7 % of

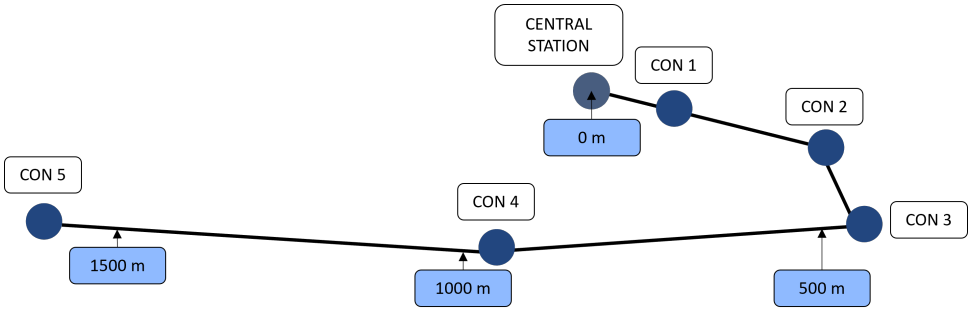

Figure 1: Map of the network.

Table 1: Peak demand and distances between consumers. The listed distance to the first consumer is from the central station.

Consumer	Peak demand [MW]	Distance from previous consumer [m]
1	1.03	110
2	1.21	220
3	1.26	130
4	0.79	520
5	1.33	620

the peak demand. The ambient temperatures were taken as hourly averages of measured weather data in 2018 to 2022 from the location of the five consumers in Denmark (Danish Meteorological Institute, 2023). The yearly temperature profile is shown in Figure 2a. The load duration curve for the entire network is shown in Figure 2b. Each consumer was assumed to have a water system to distribute space cooling (SC) throughout the building to avoid additional precautions of using R-744 directly in the buildings. The forward and return temperatures of the cooling water are provided in Table 2.

2.2 Network

The network consists of two pipelines – one for liquid R-744 and one for gaseous R-744. To avoid bubble formation in the liquid line, the R-744 is in a subcooled state and at a pressure above the saturation pressure corresponding to ambient temperature. Similarly, droplet formation in the gaseous line was avoided by keeping the R-744 in a superheated state throughout the gaseous line. Therefore, the pressure of the gaseous line should be below that of the saturation pressure corresponding to ambient temperature.

In a cooling network, the liquid line is the forward line while the vapour line is the return line (see Figure 3). When cooling should be provided at a consumer, liquid R-744 is extracted from the main liquid pipeline and sent through the substation where it is first throttled through an isenthalpic expansion to the pressure of the gaseous line. Heat is transferred from the water loop in the building to the R-744, which causes the R-744 to evaporate. The R-744 then enters the main gaseous pipeline. This leads to the central station where heat is discharged so the energy balance of the network can be maintained. In the central station, the gaseous R-744 is condensed and liquid R-744 is pumped to the liquid line. The

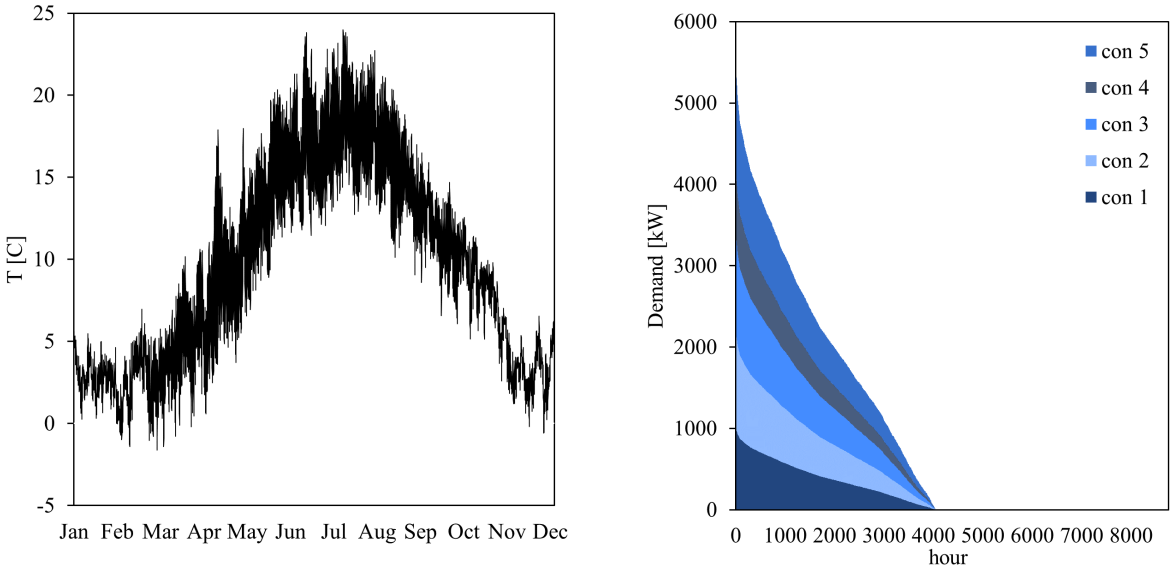

(a) Ambient temperature profile.

(b) Load duration curve of each consumer.

Figure 2: Yearly data used as basis for operation.

Table 2: Assumed parameters used in the model.

Parameter	Symbol	Unit	Value	Source
Central station				
District heat forward temperature	$T_{\mathrm{DH,for}}$	°C	80	Case specific
District heat return temperature	$T_{\mathrm{DH,ret}}$	°C	40	Case specific
Lorenz efficiency of central heat pump	$\eta_{\mathrm{cen,Lorenz}}$	%	40	Liso and Bojesen (2019)
Isentropic efficiency of liquid pump	η_{s}	%	60	Woods (2007)
Consumer substation				
Space cooling forward temperature	$T_{\mathrm{SC,for}}$	°C	12	Case specific
Space cooling return temperature	$T_{\mathrm{SC,ret}}$	°C	18	Case specific
Carnot efficiency of consumer heat pump	$\eta_{\mathrm{con,Carnot}}$	%	50	Gasser *et al.* (2017)
Pinch point in heat exchangers	ΔT_{pp}	K	5	Woods (2007)
Superheat at consumer substation	ΔT_{sh}	K	5	Case specific
Pipelines				
Maximum pressure drop in liquid line	Δp_{max}	bar	5	Case specific
Absolute roughness of internal pipe wall	$\varepsilon_{\mathrm{abs}}$	mm	0.046	White (2016)
Soil conductivity	k_{soil}	W (mK)$^{-1}$	2.4	Skaugen *et al.* (2016)
Pipe burial depth	z	m	0.9	Nagano *et al.* (2021)
Maximum liquid velocity	$u_{\mathrm{max,L}}$	m s^{-1}	2	Henchoz *et al.* (2016)
Maximum vapour velocity	$u_{\mathrm{max,G}}$	m s^{-1}	5	Weber and Favrat (2010)
Yield strength	σ_{y}	MPa	483	Lu *et al.* (2020)
Tensile strength	σ_{t}	MPa	565	Lu *et al.* (2020)

heat is discharged to the existing district heat network using a heat pump.

The central heat pump was modelled using the coefficient of performance (COP). A Lorenz efficiency (see Table 2) was used to relate the performance of the heat pump to the temperature levels at which it operated, according to Equation (1), using the entropic mean temperature of the district heat water ($\bar{T}_{\mathrm{DH}}$) and the condensation temperature of R-744 at the central station (T_{cen}). This methodology is less accurate compared to a complete cycle model, however, it can illustrate the effects of varying operating

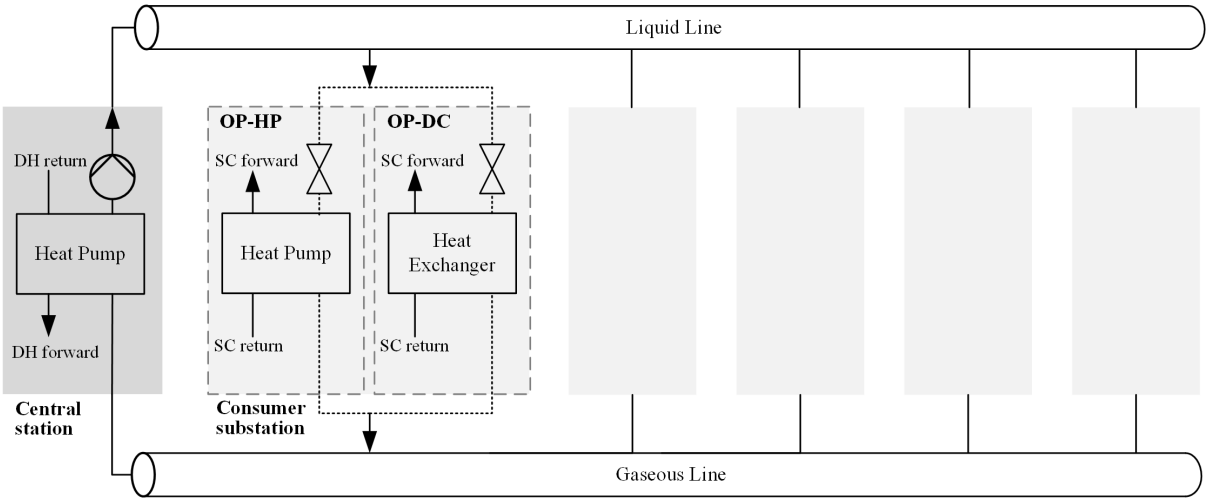

Figure 3: Process flow diagram of the system illustrating the two alternative cases (OP-HP and OP-DC).

conditions throughout the year at significantly lower computational effort. The assumed temperatures of the district heat water and the isentropic efficiency of the liquid pump are given in Table 2.

$$\mathrm{COP}_{\mathrm{cen}} = \eta_{\mathrm{cen,Lorenz}} \mathrm{COP}_{\mathrm{Lorenz}} = \eta_{\mathrm{cen,Lorenz}} \left(\frac{\bar{T}_{\mathrm{DH}}}{\bar{T}_{\mathrm{DH}} - T_{\mathrm{cen}}} \right) \tag{1}$$

In the first case (OP-HP), the temperatures of R-744 were close to ambient throughout the network. This required the use of a heat pump in the consumer substations. It was modelled using a COP and Carnot efficiency (see Table 2) to reflect changes in the heat pump performance due to different R-744 temperatures throughout the year. The COP was modelled using the evaporation temperature of R-744 in the consumer substation (T_{con}) and the evaporation temperature of the refrigerant in the heat pump given from the return temperature of the cooling water ($T_{\mathrm{SC,ret}}$), superheat of the refrigerant (10 K) and a minimum temperature approach (5 K) as given in Equation (2).

$$\mathrm{COP}_{\mathrm{con}} = \eta_{\mathrm{con,Carnot}} \mathrm{COP}_{\mathrm{Carnot}} = \eta_{\mathrm{con,Carnot}} \left(\frac{T_{\mathrm{SC,ret}} - 15\,\mathrm{K}}{T_{\mathrm{con}} - (T_{\mathrm{SC,ret}} - 15\,\mathrm{K})} \right) \tag{2}$$

The pressure (p) of the liquid line (L) at the central station (cen) was set to allow for a maximum pressure drop (see Table 2) as given in Equation (3). The liquid line pressure was defined in the same way for both operating cases.

$$p_{\mathrm{L,cen}} = p_{\mathrm{sat}}(T_{\mathrm{amb}}) + \Delta p_{\mathrm{max}} \tag{3}$$

The pressure of the gaseous line (G) was determined at the last consumer (N). In the OP-HP case, it was set to ensure a superheated state throughout the network as given by Equation (4). The superheat set point (see Table 2) was the same at all consumer substations.

$$\mathrm{OP-HP}: \; p_{\mathrm{G,N}} = p_{\mathrm{sat}}(T_{\mathrm{amb}} - \Delta T_{\mathrm{sh}}) \tag{4}$$

In the second case, OP-DC, direct cooling was provided at the consumer. The pressure of the gaseous line was then based on the supply temperature of cooling water according to Equation (5), with the assumed pinch point temperature difference given in Table 2.

$$\mathrm{OP-DC}: \; p_{\mathrm{G,N}} = p_{\mathrm{sat}}(T_{\mathrm{SC,for}} - \Delta T_{\mathrm{pp}}) \tag{5}$$

Throughout the pipelines, pressure losses and heat transfer with the ambient occurred. The pressure losses were modelled for nearly incompressible flows. It was assumed that all pipelines were placed horizontally, therefore, only losses associated with friction was included. The friction factor (f) was determined from the White-Colebrook law given in Equation (6) (White, 2016) using the Reynolds number (Re) and the relative roughness of the internal pipe surface ($\varepsilon_{\mathrm{rel}}$). This was given from the absolute roughness (see Table 2) and the internal pipe diameter (D_{i}).

$$\frac{1}{\sqrt{f}} = -2\log\left(\frac{\varepsilon_{\mathrm{rel}}}{3.71} + \frac{2.51}{\mathrm{Re}\sqrt{f}} \right) \quad \text{with} \quad \varepsilon_{\mathrm{rel}} = \frac{\varepsilon_{\mathrm{abs}}}{D_{\mathrm{i}}} \tag{6}$$

The pressure losses associated with friction in a pipe segment were then given by Equation (7), using the inlet density (ρ), flow velocity (u), and length of the pipe (L).

$$\Delta p = \frac{1}{2} \rho u^2 f \frac{L}{D_i} \tag{7}$$

Heat losses to the ambient could occur when the temperature of the R-744 was above the ambient temperature, while heat ingress occurred at flow temperatures below ambient. The overall heat transfer coefficient for each pipe segment (UA) was used to estimate the heat transfer with ambient ($\dot{Q}$) as given in Equation (8), where the temperature difference was taken as the arithmetic mean of the temperature difference at the inlet and outlet of the pipe segment.

$$\dot{Q}_{\mathrm{amb}} = UA\Delta T \quad \text{with} \quad \Delta T = \frac{(T_{\mathrm{amb}} - T_{\mathrm{in}}) + (T_{\mathrm{amb}} - T_{\mathrm{out}})}{2} \tag{8}$$

The thermal conductance was given from the total thermal resistance (R), see Equation (9). This was estimated by the thermal resistance of the soil, as this contribution was significantly greater than resistances through the pipe wall and due to internal convection in the pipe. Two-dimensional heat transfer through the soil was assumed and modelled using a shape factor (S_f), the thermal conductivity of soil (k), and the assumed burial depth (z) (see Table 2), as given in Equation (10) (Incropera *et al.*, 2017).

$$UA = \frac{1}{R_{\text{tot}}} \tag{9}$$

$$R_{\text{tot}} \approx R_{\text{soil}} = \frac{1}{S_f k_{\text{soil}}} \quad \text{with} \quad S_f = \frac{2\pi L}{\ln\left(4z/D_{\text{o}}\right)} \tag{10}$$

The dimensions of the pipes were determined based on the maximum allowed flow velocities (see Table 2) and to ensure that the pipes could withstand the maximum pressure. Therefore, the pipelines were dimensioned for the peak hour of the year, where the highest mass flow rate of R-744 was needed and the highest ambient temperature occurred, resulting in the highest pressure level within the pipelines. The diameter was chosen as the smallest possible diameter which could ensure that the required mass flow rate of R-744 did not exceed the maximum allowed velocity. The thickness (t) of the pipe wall was given from Barlow's formula shown in Equation (11).

$$t = \frac{p_{\max} D_i}{2\sigma_{\max}} \tag{11}$$

The maximum allowed stress (σ) of the material could not exceed the guidelines from the Council directive 2014/68/EU (2014) given in Equation (12). The pipes were assumed to be of API 5L X70 steel, and the assumed yield (y) and tensile (t) strengths are given in Table 2. The pipe dimensions were chosen among existing standard Nominal Pipe Sizes (NPS) (ASME, 2018).

$$\sigma_{\max} = \text{Min}\left(\frac{2}{3}\sigma_{\text{y}}, \frac{5}{12}\sigma_{\text{t}}\right) \tag{12}$$

3 RESULTS

3.1 System design

Different pipe dimensions were needed for the liquid side in the two cases. The case using heat pumps at the consumer substation (OP-HP) generally required larger pipe diameters (see Table 3) and thicker pipe walls to some extend. This was caused by the need for higher mass flow rates of R-744 in the OP-HP case, as the R-744 should also receive the energy transferred to the heat pump compressors in the consumer substations. The pipe sizes of the gaseous line were not affected by the different operating strategies. In the case where direct cooling was provided (OP-DC), the temperature levels of the gaseous line were lower, meaning a slight increase of the density. Therefore, the volume flow rate did not show significant changes and the same pipe sizes were needed to achieve a lower mass flow rate compared to the OP-HP case.

Table 3: Outer diameter and wall thickness of pipe segments on the liquid and gas side of the network for the two different operating cases.

		OP-HP					**OP-DC**				
Pipe segment		**1**	**2**	**3**	**4**	**5**	**1**	**2**	**3**	**4**	**5**
D_{o} **[mm]**	**L**	194	168	141	114	89	168	141	114	102	89
	G	273	245	219	168	141	273	245	219	168	141
t **[mm]**	**L**	7.6	2.8	2.8	2.1	2.1	2.8	2.8	2.1	2.1	2.1
	G	3.4	8.7	2.8	2.8	2.8	3.4	8.7	2.8	2.8	2.8

In the design point, the liquid and gaseous lines were operated at lower pressures in the OP-DC case compared to the OP-HP case. Therefore, a greater pressure lift should be provided by the central liquid pump increasing the power consumption (see Table 4). Furthermore, it affected the operation of the central heat pump, which operated at a greater temperature lift, resulting in higher power consumption. Since the power consumption of the liquid pump and central heat pump were greater, the total nominal heat discharged to the district heat network was slightly greater for the OP-DC case (see Table 4). This was the case even though the cooling at the consumers were provided using power consuming heat pumps in the OP-HP case.

The results show, that larger pipes will be needed for the OP-HP case. Together with the need of heat pumps at the consumer substations, this will likely result in greater capital investment compared to the OP-DC case for this part of the system. However, the central station required a heat pump and a liquid pump with slightly greater capacity for the OP-DC case. This could increase the capital investment.

3.2 Yearly Operation

In hours with high ambient temperature, the temperatures through the pipelines were greater for the OP-HP case compared to OP-DC (see Figure 4) for both the liquid and gaseous lines. As the ambient temperature reduced, the temperature levels of the two operating cases approached each other. The different operating temperatures affected the heat transfer with ambience (see Figure 5). This resulted in significantly less heat ingress for the OP-HP case. As the ambient temperature reduced throughout the year, similar heat transfer with ambient in the two cases occurred. The total yearly cooling demand was 8478 MWh and the total heat ingress over a year amounted to 79 MWh and 231 MWh for the OP-HP and OP-DC case, respectively (see Table 5). The major benefit of operating close to ambient temperatures occurred during the warm hours, where the heat ingress in the liquid line could be reduced more than 50 % of the OP-DC case (see Figure 5a). Even greater reductions were achieved for the gaseous line (see Figure 5b), where the heat loss was almost eliminated when operating close to ambient temperatures. The heat ingress corresponded to 1 % (OP-HP) and 3 % (OP-DC) of the total cooling demand. This indicates, that in both cases, the heat ingress was of minor importance.

Throughout the year, the pressure level at the liquid line inlet in the central station was defined in the same way for both cases and it followed the reduction in ambient temperature (see Figure 6). The pressure level at the inlet to the gaseous line from the last consumer in the network were constant in the OP-DC case, while it followed ambient temperature in the OP-HP case. In hours with relatively low temperatures, the pressure levels were close to equal (see Figure 6). The pressure losses in the pipelines were in the same size order throughout the year (see Figure 7). In the warmest hours, a slightly greater total pressure loss occurred in the OP-HP case. This was caused by the gaseous line and the longest

Table 4: Nominal power consumption and district heat production of the system for the two different operating strategies.

	$\dot{W}_{\mathrm{HP,con}}$ kW	$\dot{W}_{\mathrm{pump,cen}}$ kW	$\dot{W}_{\mathrm{HP,cen}}$ MW	$\dot{Q}_{\mathrm{DH}}$ MW
OP-HP	618	101	2.8	9.1
OP-DC	–	127	3.5	9.4

Table 5: Yearly power consumption, district heat production, heat ingress of the system for the two different operating strategies.

	$\dot{W}_{\mathrm{HP,con}}$ MWh	$\dot{W}_{\mathrm{pump,cen}}$ MWh	$\dot{W}_{\mathrm{HP,cen}}$ MWh	$\dot{Q}_{\mathrm{DH}}$ MWh	$\dot{Q}_{\mathrm{amb,L}}$ MWh	$\dot{Q}_{\mathrm{amb,G}}$ MWh
OP-HP	558	106	4886	14 106	74	5
OP-DC	–	131	5573	14 414	142	89

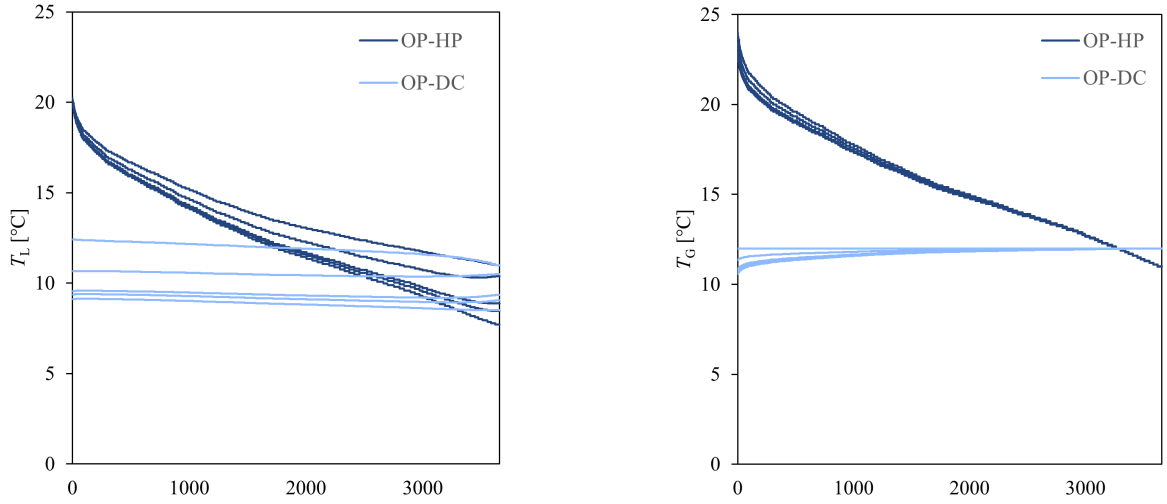

(a) Liquid line. **(b)** Gaseous line.

Figure 4: Yearly temperature levels (hour 1 is at peak load and highest ambient temperature).

liquid pipe segment (to consumer five) having the same diameter in both cases (see Table 3). However, larger mass flow rates and hence velocities were required in the OP-HP case, resulting in greater pressure losses. In colder hours, where demand decreased, the mass flow rates were reduced relatively more for the OP-HP case as the discharge of energy to the R-744 from the consumer heat pump compressor also decreased. This resulted in lower velocities in the liquid pipelines with greater diameters (pipe segment one to four) in the OP-HP case and lower pressure losses compared to the OP-DC case.

The pressure difference between the liquid and gaseous line were approximately constant throughout the year in the OP-HP case (see Figure 6), resulting in the power consumption of the central liquid pump following the reduction in mass flow rate (see Figure 8a). The power consumption for the liquid pump also decreased for the OP-DC case but to a greater extend, as the pressure lift provided by the pump also decreased. The yearly power consumption of the pump was 24 % greater for the OP-DC case compared to the OP-HP case (see Table 5). The power consumption of the central heat pump providing district

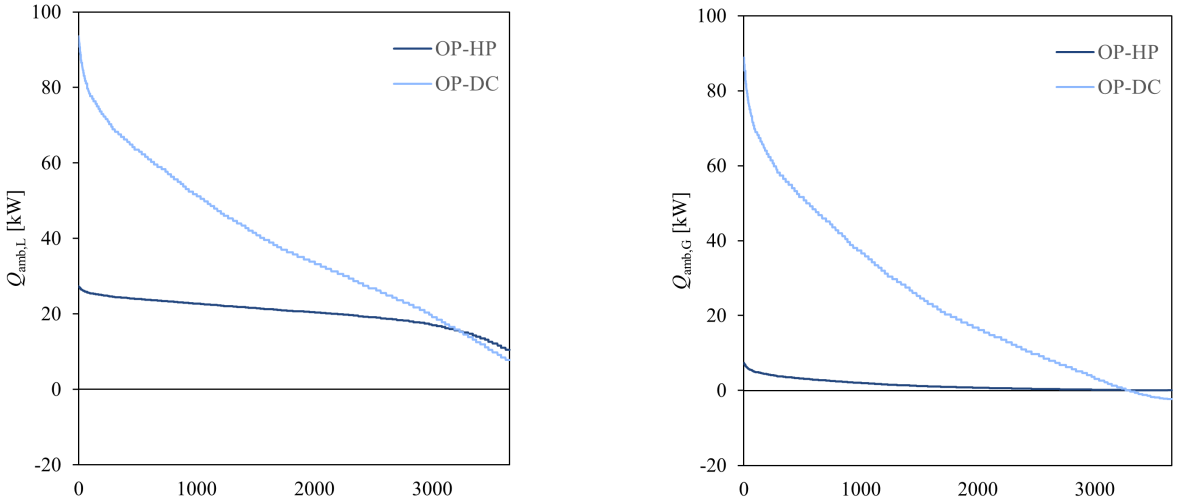

(a) Liquid line. **(b)** Gaseous line.

Figure 5: Yearly heat transfer with ambient (hour 1 is at peak load and highest ambient temperature).

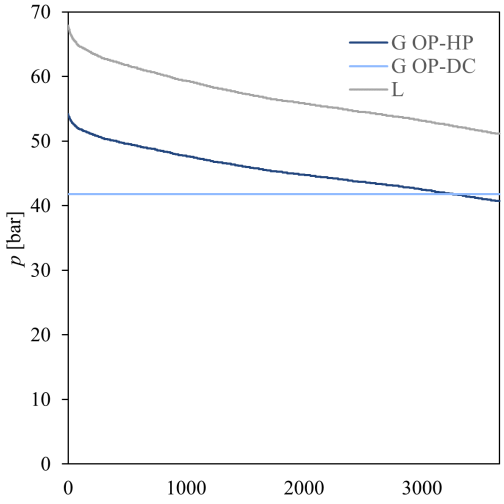

Figure 6: Pressure level set points. Liquid line pressure was set similar for both cases.

heat also reduced throughout the year for both operating cases (see Figure 8b). This was caused by a reduction in the cooling demand and the amount of heat that should be discharged. The reduction in power consumption was less steep for the OP-HP case, because the pressure level of the gaseous line, and hence the condensation temperature of R-744 at the central station was reduced in hours with lower ambient temperature. This reduced the COP of the heat pump, resulting in a higher power consumption per unit of discharged heat. The total yearly power consumption of the central heat pump was 14 % greater for the OP-DC case than the OP-HP case.

The total yearly power consumption of the OP-HP case amounted to 5.55 MWh while it was 5.70 MWh for the OP-DC case. The OP-DC case had a greater power consumption because the central heat pump operated at a lower COP for most of the hours throughout the year. However, this also resulted in a slightly greater production of district heat (see Table 5). The results of the yearly operation show, that the two cases had similar total power consumption, only with the OP-DC case showing a slightly greater consumption of 3 %. Approximately the same district heat was produced in the two cases. The

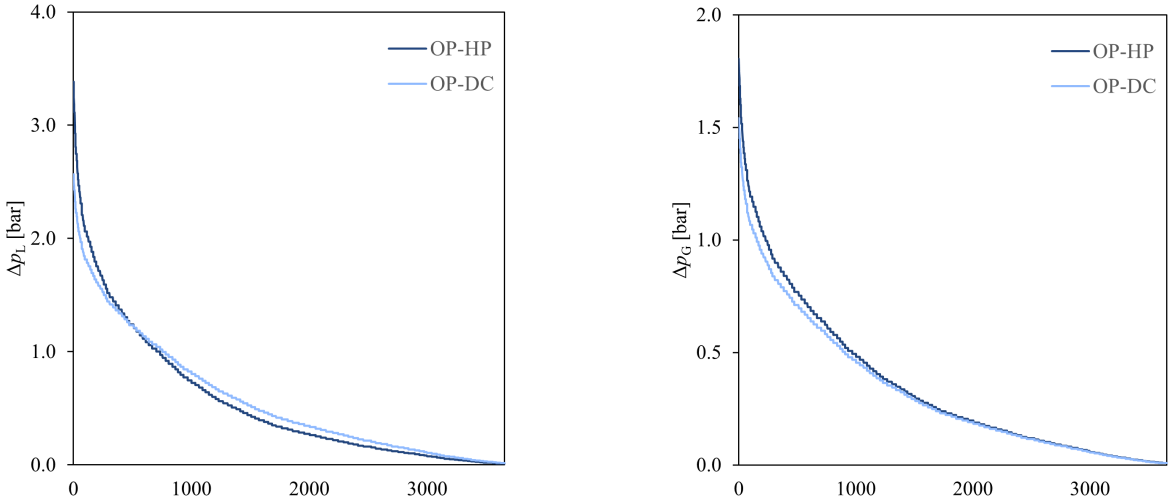

(a) Liquid line.

(b) Gaseous line.

Figure 7: Yearly pressure losses (hour 1 is at peak load and highest ambient temperature).

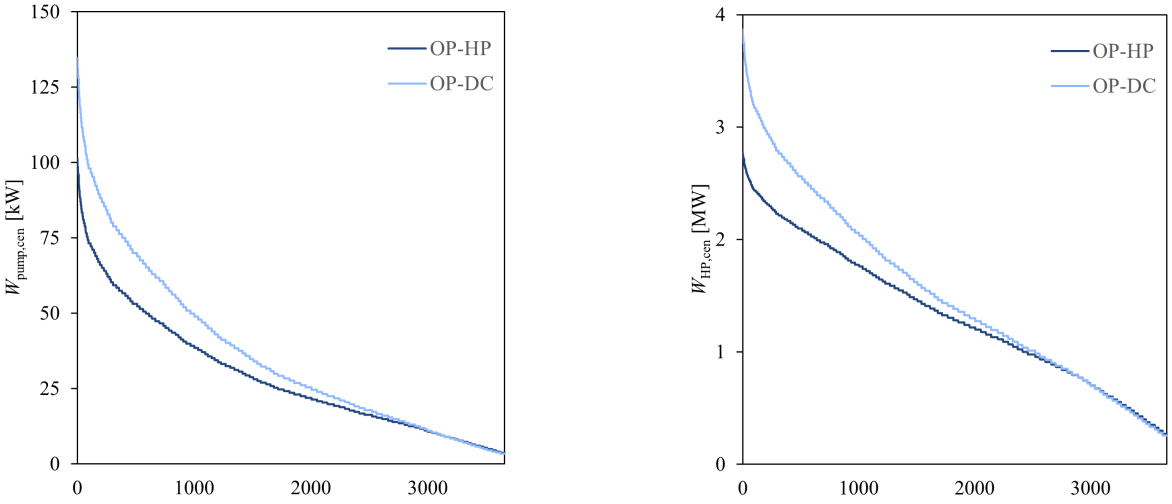

(a) Central pump. **(b)** Central heat pump.

Figure 8: Yearly power consumption (hour 1 is at peak load and highest ambient temperature).

greatest differences in operation occurred in the warmest hours of the year, as the temperature levels of the OP-HP case approached the OP-DC case as the ambient temperature decreased, resulting in similar operating conditions.

4 DISCUSSION

The two alternative set points of pressure levels through the gaseous line affected different aspects of the network. Trade-offs between the pipelines, consumer substation, and the central station were seen. Providing direct cooling resulted in the need of smaller liquid pipelines and can likely reduce the capital investment of the consumer substation. Furthermore, no power is consumed in the consumer substation. However, a larger central heat pump was needed and additional power was consumed by the central station, as the COP of the heat pump (assuming the same Lorenz efficiency) was lower and a greater pressure lift was supplied through the liquid pump. It is possible that a better COP could be achieved for the central heat pump in the OP-DC case, but this would likely increase capital investment. These costs of the network might be distributed between the network operators and the consumers. Assuming that the consumers would be charged higher costs when using a heat pump in the consumer substations, it would likely be more economically beneficial to have direct cooling. From the operators view, it is a question of the trade-offs between the capital costs of pipelines and central station and the operating costs associated with the central station. Furthermore, the production of district heat is associated with a revenue which will be greater for the case of providing direct cooling. The most economically beneficial system might therefore depend on whether a socio- or private-economic analysis is adopted.

If a natural heat sink was available, this could be used at the central station in a similar way as by Weber and Favrat (2010) and Nagano *et al.* (2021). It would make the central heat pump redundant, which could significantly reduce the power consumption of the network. In such case, the OP-HP case would have a power consumption of 664 MW on a yearly basis, while the OP-DC would consume 131 MW. However, the heat discharged from the network would not collect revenue from district heating sales. Alternatively, the consumers could be provided with heating directly by the R-744 network (as proposed by Weber and Favrat (2010)). Furthermore, this could reduce the number of pipelines needed for the district heating and cooling systems as a whole. In any case, the investigated R-744 based district cooling systems required smaller pipelines compared to regular water based systems.

5 CONCLUSION

A thermodynamic model was made of a district cooling system using R-744 as the energy carrier. The system was used to supply comfort cooling to five commercial consumers throughout the year according to varying ambient temperatures. The heat from the network was discharged to the local district heat network using a heat pump. The system was designed and operated in two alternative ways. First, the network was operated close to ambient temperature, resulting in the need of heat pumps at the consumer substations to provide adequate cooling. Second, the network was operated at a temperature level sufficiently low for providing direct cooling at the consumers. The system with direct cooling required smaller pipe sizes in the forward lines of the network, which could likely reduce the capital investment of the network. However, a larger central heat pump was needed. The yearly power consumption was found to be slightly higher for the case of direct cooling, due to worse performance of the central heat pump. If the heat could be discharged to a natural reservoir at appropriate temperature levels, there would be significant reduction in power consumption from using direct cooling compared to the heat pump case. The heat ingress from ambient did not show to be significant in any of the two cases. The results show, that the operating strategy of pressure levels in the system should be chosen not only to optimise the consumer substation but should also consider the operation of the central heat pump, as this is an important component of both operation and capital expenses.

ACKNOWLEDGEMENT

This article comes out of the CO2inLOOP project under the ERANET scheme of the Horizon Europe program financially supported by Innovation Fund Denmark (Case Number: 1158-00010B).

NOMENCLATURE

Roman Letters

$\dot{Q}$	Heat transfer rate [kW]
D	Diameter [m]
f	Friction factor [–]
k	Conductivity [W (m K)$^{-1}$]
L	Lenght of pipe segment [m]
p	Pressure [bar]
R	Thermal resistance [K kW^{-1}]
S_f	Shape factor [m]
T	Temperature [°C]
t	Thickness of pipewall [m]
u	Velocity [m s^{-1}]
UA	Thermal conductance [kW K^{-1}]
z	Burial depth [m]

Greek Letters

η	Efficiency [%]
ρ	Density [kg m^{-3}]
σ	Strength [MPa]
ε	Surface roughness [m]

Subscripts and superscripts

amb	Ambient
cen	Central
con	Consumer
cw	Cooling water
for	Forward
G	Gaseous line
i	Inner
L	Liquid line
N	Number of consumers
o	Outer
pp	Pinch point
ret	Return
s	Isentropic

sat	Saturation
sh	Superheat
t	Tensile
y	Yield

Abbreviations

COP	Coefficient of performance
DC	Direct cooling
DH	District heat
HP	Heat pump
OP	Operation strategy
SC	Space cooling

REFERENCES

ASME. (2018). *Welded and seamless wrought steel pipe b36.10*.

Council directive 2014/68/EU. (2014). On the harmonisation of the laws of the member states relating to the making available on the market of pressure equipment. https://data.europa.eu/eli/dir/2014/68

Danish Meteorological Institute. (2023). *DMI open data portal. version 1.30.18* [accessed 07/12/2023]. https://dmiapi.govcloud.dk/

Gasser, L., Flück, S., Kleingries, M., Meier, C., & Bätschmann, M. (2017). High efficiency heat pumps for low temperature lift applications. *12th International Heat Pump Conference*.

Henchoz, S., Favrat, D., Marechal, F., & Girardin, L. (2017). Novel district heating and cooling energy network using CO_2 as a heat and mass transfer fluid. *12th IEA Heat Pump Conference*.

Henchoz, S., Chatelan, P., Maréchal, F., & Favrat, D. (2016). Key energy and technological aspects of three innovative concepts of district energy networks. *Energy*, *117*, 465–477. https://doi.org/10.1016/j.energy.2016.05.065

Henchoz, S., Weber, C., Maréchal, F., & Favrat, D. (2015). Performance and profitability perspectives of a CO_2 based district energy network in Geneva's City Centre. *Energy*, *85*, 221–235. https://doi.org/10.1016/j.energy.2015.03.079

IEA. (2018). *The future of cooling* (License: CC BY 4.0). https://www.iea.org/reports/the-future-of-cooling

Incropera, F. P., Dewitt, D. P., & Bergman, T. L. (2017). *Incroperas principles of heat and mass transfer* (8th). Wiley.

Intergovernmental Panel on Climate Change. (2022). *Mitigation pathways compatible with 1.5°C in the context of sustainable development*. Cambridge University Press. https://doi.org/10.1017/9781009157940.004

Liso, V., & Bojesen, C. (2019). Assessment of heat pumps for district heating applications. *CUE2019 Applied Energy Symposium*.

Lu, H., Ma, X., Huang, K., Fu, L., & Azimi, M. (2020). Carbon dioxide transport via pipelines: A systematic review. *Journal of Cleaner Production*, *266*. https://doi.org/10.1016/j.jclepro.2020.121994

Nagano, T., Kajita, J., Yoshida, A., & Amano, Y. (2021). Estimation of the utility value of unused heat sources for a CO_2 network system in Tokyo. *Energy*, *226*. https://doi.org/10.1016/j.energy.2021.120302

Ritchie, H., & Roser, M. (2020). *CO_2 and greenhouse gas emissions*. https://ourworldindata.org/greenhouse-gas-emissions

Skaugen, G., Roussanaly, S., Jakobsen, J., & Brunsvold, A. (2016). Techno-economic evaluation of the effects of impurities on conditioning and transport of CO_2 by pipeline. *International Journal of Greenhouse Gas Control*, *54*, 627–639. https://doi.org/10.1016/j.ijggc.2016.07.025

Weber, C., & Favrat, D. (2010). Conventional and advanced CO_2 based district energy systems. *Energy*, *35*, 5070–5081. https://doi.org/10.1016/j.energy.2010.08.008

White, F. M. (2016). *Fluid mechanics* (8th). McGraw-Hill Education.

Woods, D. R. (2007). *Rules of thumb in engineering practice*. Wiley-VCH Verlag GmbH & Co.